Dynamic power allocation of battery-supercapacitor hybrid energy storage for standalone PV microgrid applications

Dynamic Power Allocation of Battery-Supercapacitor Hybrid Energy Storage for Standalone PV Microgrid Applications

Wenlong Jing[a]*, *Chean Hung Lai*[a], *Wallace S.H. Wong*[a]
[a]Faculty of Engineering, Computing and Science, Swinburne University of Technology Sarawak Campus, Jalan Simpang Tiga, 93350 Kuching, Sarawak, Malaysia

M. L. Dennis Wong[b]
[b]School of Engineering and Physical Sciences, Heriot-Watt University (Malaysia Campus), Putrajaya, Malaysia

*Corresponding author: wjing@swinburne.edu.my

***Abstract* —** Standalone photovoltaic-based microgrid with energy storage system could be a promising solution for powering up off-grid communities. One of the major issues that hinder the development of standalone microgrids is the poor service life of the batteries. To address this issue, hybrid energy storage systems (HESS) and novel power management strategies have been proposed by researchers to enhance the service life of battery bank. This paper presents a novel multi-level hybrid energy storage system topology and its associated power management strategy to mitigate the charge/discharge stress on battery. Matlab Simulink model of typical standalone PV microgrid with different HESS topologies are developed to evaluate the performance of the proposed system. Actual solar irradiance data with different weather conditions and estimated load profile based on site survey results are used to analyze the effectiveness of different HESS in mitigating stress on batteries. A comprehensive analysis and benchmarking is presented to compare the technical and financial viability of the proposed system with existing HESS solutions. Simulation results show that the proposed HESS can improve the life expectancy of the battery and reduce the operating cost of the standalone PV-Battery microgrid.

Keywords *– photovoltaic, microgrid, renewable energy, hybrid energy storage, energy management, rural electrification.*

1. INTRODUCTION

The greenhouse effect is well understood via many research works and its increasing emissions are leading to a global environmental deterioration in recent years [1]. To reverse these undesirable scenarios, as a replacement to traditional fossil energy sources, renewable energy sources could play an important role in the future power systems [2]. According to [3], nearly 1.2 billion people of the global population lacked electricity till to 2016 and it will be projected to decline to around 12 percent by 2030. More than 80 percent of these people live in remote rural areas without reliable electricity supply. Standalone microgrid with renewable energy sources could be an attractive solution to address the electricity needs in these remote communities. Currently, the major sources of renewable energy include wind, photovoltaic (PV), hydrogen fuel cells, tidal, and geothermal energy. Among these renewable technologies, PV microgrid is one of the attractive options for low density off-grid communities. For example, the remote longhouses located at the inner region of Sarawak, Malaysia.

Fig. 1 illustrates a typical output power profile of solar energy in Sarawak and an estimated energy consumption pattern of rural communities. The relatively low capacity load demand and intermittent nature of solar energy cause extreme fluctuation in power generation and load, leading to severe imbalance in the power network. Therefore, energy storage system (ESS) is generally required in renewable-based microgrid system to act as a buffer between generation and load [4]. ESS increases energy utilization by mitigating the temporal mismatch between PV power generation and load demand by storing surplus energy during peak power generation period and provide the stored energy to the load during generation off-peak [5]. In addition, ESS in

PV Microgrid also plays an important role in compensating the reactive power as well as suppressing the voltage fluctuation and flicker [6].

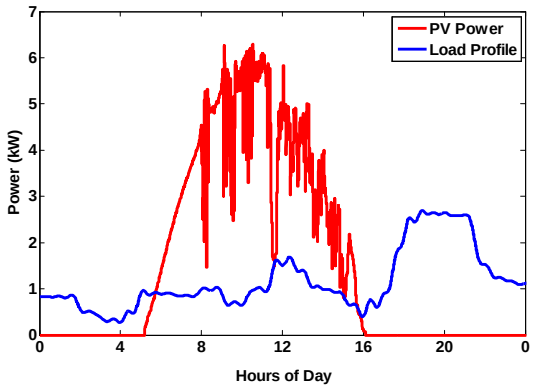

Fig. 1. Typical PV output power and load profile in rural Sarawak, Malaysia.

Among many ESS devices available on the market, lead acid (LA) batteries have been the mainstream residential energy storage solutions. LA battery is a matured and well understood energy storage technology which is robust and low cost. However, the main drawback of LA batteries is the short cycle life especially when it is operated in cycling applications [7]. The main life-limiting factors of LA battery such as high charge/discharge rate, overcharge, high depth-of discharge and dynamic loading pattern are all commonly experienced in PV-based residential energy storage system [8]. A typical LA battery may only last for hundreds of charge/discharge cycles which make it economically unsustainable as the ESS being the main cost component in typical PV-based Microgrids [9].

To address these shortcomings, hybrid energy storage system (HESS) has been proposed by many researchers [10]–[14]. HESS exploits the strength of different ESS devices to compensate weaknesses of homogenous storage element. Many research studies have demonstrated that HESS could reduce the internal system losses and relieve the battery charging/discharging stress which leads to prolonged battery life [15]–[18]. *Glavin et. al.* have verified that SC-battery HESS performs better than battery-alone energy storage system in standalone PV microgrids [19]. *Dougal et al.* mathematically proved that the HESS is capable of extending the battery lifetime [20]. *Anthony et al*. used a small-scale wind energy prototype system to demonstrate the improvement in battery lifetime when using SCs [15].

The main idea of HESS is to direct the damaging loading conditions such as severe fluctuation in charge/discharge current to a more robust ESS device. Ideally, the primary battery bank should be responding to the averaged energy exchange due to the mismatch of the generation and demand. To achieve the desired power allocation to different ESS elements, actively controlled bidirectional DC/DC converters are required alongside with the optimally designed energy management system (EMS). In general, there are two objectives when designing the EMS for power sharing among different ESS elements: (1) to improve power quality and energy efficiency and (2) to prolong the lifetime of ESS [21].

Among many HESS configurations, SC-battery HESS have been one of the most popular combinations in microgrid applications [16], [22]–[24]. Bidirectional dual active bridge DC/DC converters were used to enable dynamic power allocation to the battery bank and SC respectively [22]. The authors claimed that the HESS permits online battery replacement and allows changing of the battery configuration without disturbing the system normal operation. However, this topology requires a large number of individual DC/DC converters that dramatically increase the system complexity and overall cost. *Kollimalla et. al.* presented an actively controlled SC-battery HESS topology with novel EMS that monitors the demand-generation mismatch and utilizes the error component of battery current to control the SC power flow [23]. This control strategy relies heavily on the characteristics of energy storage devices and lacks of interactions among the HESS and other components in

microgrid. Thus, the control strategy tends to application oriented which may not be applicable to other systems. A SC-battery HESS with multiple SC modules was presented in [16] that demonstrated to effectively mitigate battery stress. The individually controlled SC module allows wide range of power requirements which increase the flexibility and efficiency. However, the redundant SC modules increase the overall cost and complexity. Other than SC-battery HESS, dual separate battery pack as the energy storage in which the batteries are charged by PV panels separately via two solid-state switches [25], [26].

This paper presents a novel multi-level HESS topology and its associated power management system which is developed upon the SC-battery hybridization and dual battery solution that include SC and two battery modules of different chemistries and characteristics. The low cost LA battery will be the primary ESS that makes up the system capacity, while the Li-ion battery with higher price tag but robust will be the secondary ESS that absorb medium to high frequency fluctuation. The power distribution among them is set via a scaling factor which can be varied in different scenarios. SC on the other hand, is programmed to response to high frequency power exchange. A typical Standalone PV microgrid for rural electrification is used to demonstrate the performance of the proposed HESS scheme. Comparison between Battery-Only system and common SC-battery HESS topologies is presented and discussed.

The rest of the paper is organized as follows: Section II presents the configuration of the existing HESSs and the proposed HESS for standalone PV microgrid and the corresponding power management strategies. Section III presents the numerical simulation and thorough analysis and discussion. Section IV presents the evaluation and comparison of battery stress mitigation with a novel battery health cost function. Analysis will be extended to evaluate the economic viability of the different HESS topologies. Lastly, section V concludes the paper.

2. SC-Battery HESS Topologies

In SC-battery HESS, the two ESS devices can be coupled to either a common DC or AC bus. For standalone renewable microgrid, common DC bus is the preferred choice because majority of renewable energy sources operate in DC and no synchronization is needed which minimizes the system complexity [27]. The following sections review the different SC-battery HESS topologies in common DC bus settings.

2.1. Battery-Only ESS

Conventionally, a typical DC-coupled PV microgrid is configured as shown in Fig. 2. The battery bank sits directly between the generation and load to create a relatively stable DC bus [28]. This simple structure regulates the imbalance PV generation and load demand through charging / discharging the battery bank. This conservative system performs efficiently under stable generation and demand, however fluctuation in generation and load are often the case for PV microgrid. As a result, the battery has to absorb/supply dynamically at all times, putting additional stress on the battery which could potentially accelerate cycle life.

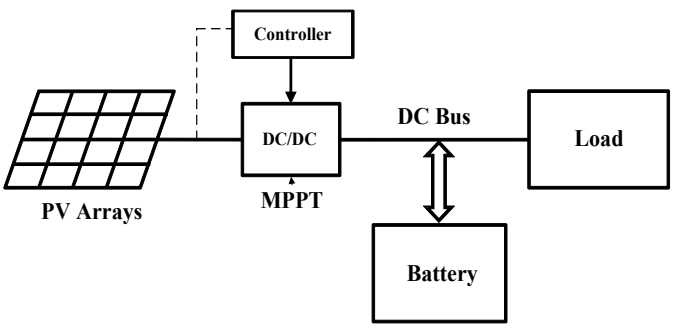

Fig. 2. PV microgrid with battery-only ESS topology.

2.2. Passive SC-Battery HESS

In recent years, researchers have been actively investigating in the SC-battery hybridization for standalone PV microgrid [29]–[31]. It is reported that by hybridizing SC and battery, the charge/discharge stress on battery can be mitigated by allocating the highly dynamic power exchange to the SC. The simplest form of SC-Battery hybrid energy storage system is to passively connect the SC and battery in parallel as illustrated in Fig.3.

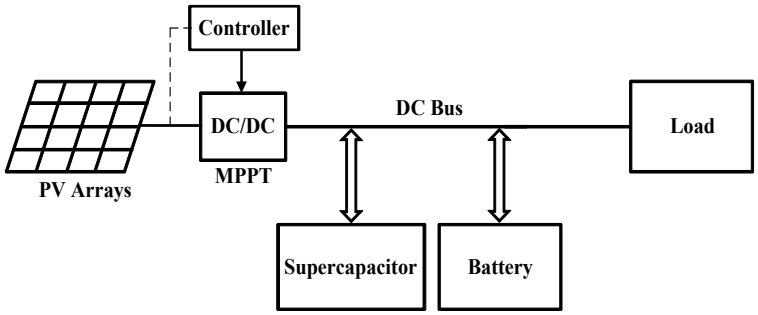

Fig. 3. PV microgrid with passive SC-battery HESS topology.

This passively connected HESS does not require any form of active control mechanism, thus reducing the implementation cost and system complexity. However, as the terminal of SC and battery are sharing the same DC bus, the configuration of HESS must be carefully designed to avoid terminal voltage mismatch. In addition, the distribution of load current is purely determined by the internal resistances and capacitance of the two ESSs. As presented in [32], the passively connected SC and battery can be modeled as an equivalent circuit model as shown in Fig. 4(a). The SC is generally modelled as a large capacitance C and an equivalent series resistance R_c, while the battery is modelled as an ideal voltage source V_b with an equivalent series resistance R_b.

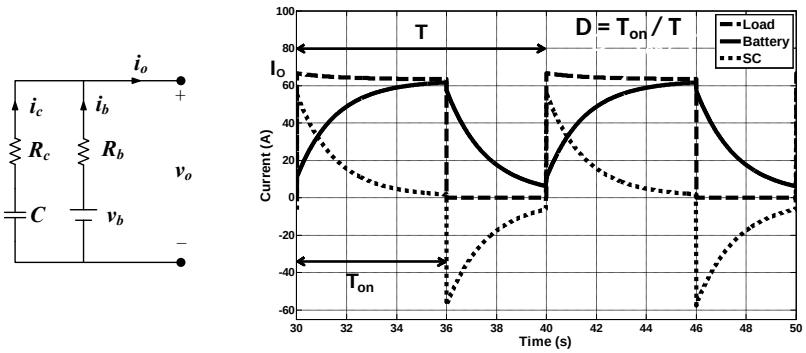

(a) (b)

Fig. 4. (a) Equivalent circuit model of passive SC-battery HESS topology; (b) Power sharing of passive HESS under periodical pulsed load.

The branch currents of the battery $i_b(t)$ and the SC $i_c(t)$ to pulsed load can be derived as [20]:

$$i_b(t) = -\frac{(V_{co} - V_b)}{R_b + R_c} * e^{-\frac{t}{(R_b + R_c)C}} + I_o \sum_{k=0}^{N-1} \left[\left(1 - \frac{R_b}{R_b + R_c} e^{-\frac{t - kT}{(R_b + R_c)C}}\right) \emptyset(t - kT) - \left(1 - \frac{R_b}{R_b + R_c} e^{-\frac{t - (k + D)T}{(R_b + R_c)C}}\right) \emptyset(t - (k + D)T) \right] \quad (1)$$

$$i_c(t) = i_0(t) - i_b(t) \quad (2)$$

Where V_{co} is the SC initial voltage, I_0 is the peak current of the pulsed load, T is the period of the pulsed load and D is the duty cycle of the pulsed load and $i_o(t)$ is the output current. From Equation (1), the power sharing between SC and battery is determined by the internal resistances R_b and R_c as well as the capacity C of the SC. Thus, the power allocation in passive HESS will be fixed throughout the entire operation of microgrid. Fig. 4(b) shows an example of the power sharing in passive HESS under periodic pulsed load. As can be seen from the simulation result in Section IV, the SC in passive HESS is under-utilized as a result of sharing identical terminal voltage with battery.

2.3. Parallel Active SC-Battery HESS

To address the low level of controllability in passively connected HESS, interfacing the ESSs using bidirectional DC/DC converters allow the power exchange of the distinct ESS elements to be fully controllable. The isolation of ESS from DC bus offers greater flexibility in HESS configuration, better volumetric efficiency and cycle life [33], [34]. Unlike passive HESS, the performance and usefulness of actively controlled HESS relies heavily on the power allocation and control strategy [35]. Therefore, a carefully designed control strategy is essential to justify the extra cost of active components.

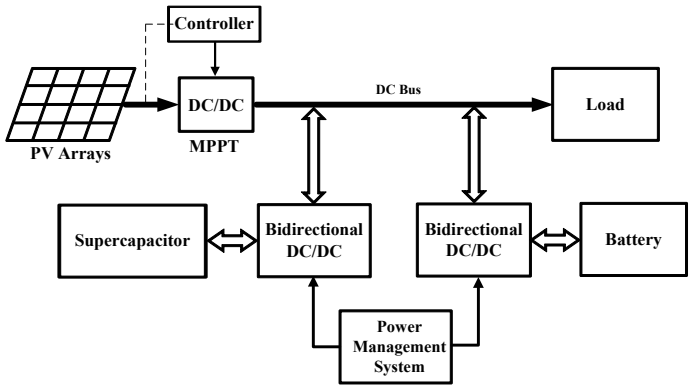

Fig. 5. PV microgrid with parallel active SC-battery HESS topology.

Fig. 5 depicts a parallel connected active HESS topology where both SC and battery are connected in parallel to DC bus via bidirectional DC/DC converters. In general, the battery as high energy density ESS is programmed to meet the low-frequency power variation throughout the day, while the SC is controlled to response to the high-frequency power exchange or to regulate the DC bus voltage.

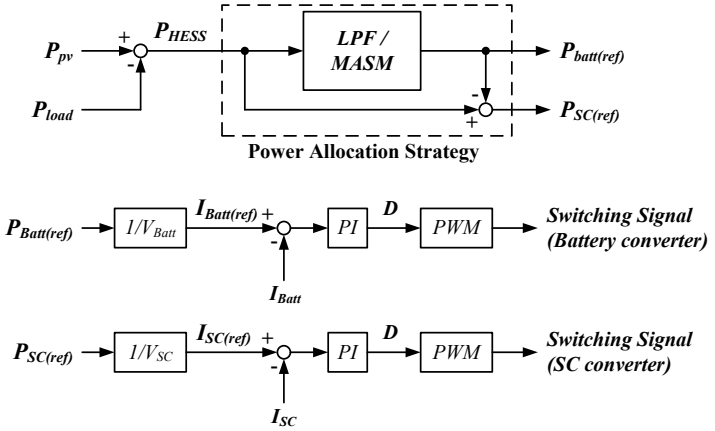

Fig. 6. Typical power allocation strategy of parallel active SC-battery HESS topology

Fig. 6 shows a typical power allocation and control strategy of parallel active HESS. Low-pass filtering (LPF) and moving average smoothing method (MASM) are commonly used power allocation strategies to decompose the low frequency component of the power demand P_{HESS} to mitigate battery stress [36], [37].

The power reference signals (P_{Batt} and P_{SC}) will pass through respective control loops with PI controller to correct the instantaneous battery current I_{Batt} and SC current I_{SC} by adjusting the duty cycle (D) of PWM signals. When selecting the bandwidth of the LPF or window size of the MASM, a tradeoff exists between smoothness of battery current I_{Batt} and SC size. For example, having a low cut-off frequency in LFP or extremely large window size in MASM generates smoothed I_{Batt} but requires extremely large SC capacity and power rating of DC/DC converter to compensate the sluggish battery response.

2.4. Proposed Multi-Level HESS

SC-battery HESS has been demonstrated to significantly mitigate battery stress under dynamic power exchange in renewable microgrid applications. However, technical and financial limitations such as SC's size and converter's power rating suppress what the HESS can potentially offer. In this work, a novel multi-level HESS topology and its power allocation strategy is proposed to address the abovementioned issues.

Fig. 7 illustrates the proposed multi-level SC-battery HESS topology for PV based microgrid. Unlike the centralized control of battery bank in conventional HESS settings, the proposed multi-level HESS splits the single battery bank into primary battery and secondary battery. The secondary battery generally holds a small portion of the overall battery capacity and it can be make up from different type of battery, for example Li-ion battery. The higher level of hybridization allows greater flexibility in power sharing among different ESS elements within the HESS.

In addition, it is possible to provide a smoother I_{Batt} (for primary battery) with the same capacity of SC compared to conventional parallel active HESS (see Fig. 5). A diesel generator as backup energy source is integrated to the ESS system in case of extreme conditions such as low battery state-of-charge due to low PV generation in rainy days or when there is big event going on in the community, for example during annual festival. The diesel generator is controlled automatically by the power management system and is designed to charge the primary battery bank when the battery state-of-charge is below 40 percent to avoid deep discharge. Conversely, the diesel generator can also be operated manually by users when a heavy consumption is expected. The analysis in this work assumes that the community keeps sufficient petrol fuel in reserve so that the electricity supply is guaranteed.

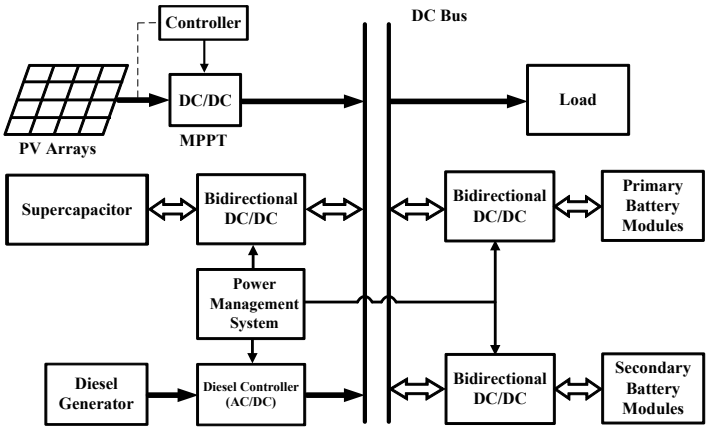

Fig. 7. Topology of the proposed multi-level HESS in standalone PV microgrid.

Fig. 8 shows the proposed multi-level power allocation strategy. Unlike conventional linear filtering or MASM approaches, the power requirement of the HESS P_{HESS} is decomposed into three frequency bands using two simple low-pass filters. The low frequency part of the power requirement will be used as the reference signal $P_{batt\_1(ref)}$ to command the primary battery, the medium frequency power exchange $P_{batt\_2(ref)}$ will be satisfied by the secondary battery, and the high frequency fluctuation $P_{SC(ref)}$ will be delivered by the SC. Since a certain portion of the battery bank will be relocated from the primary battery, same portion of the average power requirement (low frequency) will also be allocated to the secondary battery via a scaling factor W_1. In different scenarios, the scaling factor can be set manually or varied via advanced control algorithm to face the different specific conditions.

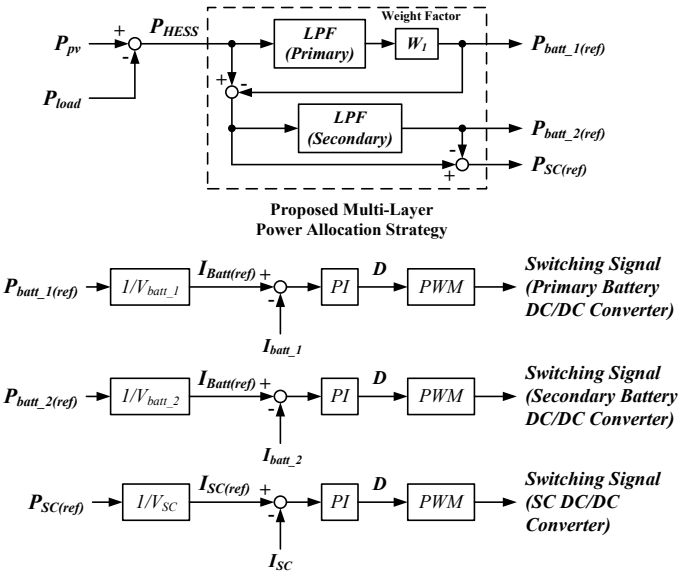

Fig. 8. Power allocation strategy for the proposed multi-level HESS in atandalone PV microgrid.

3. Numerical Analysis and Case Study

Fig. 9 shows the Matlab Simulink model of the proposed multi-level HESS. The system parameters and simulation conditions used in the analysis are tabulated in Table 1. Three bidirectional buck-boost DC/DC converters are employed to actively control the current to/flow from the primary battery, secondary battery and SC to the common DC bus. The time constants of the respective low pass filter are set to decompose the P_{HESS} to low frequency $P_{batt\_1(ref)}$ for primary LA battery bank and medium frequency $P_{batt\_2(ref)}$ for secondary Li-ion

battery bank. The remaining high frequency power exchange will be used as a reference signal to control the SC module $P_{sc(ref)}$.

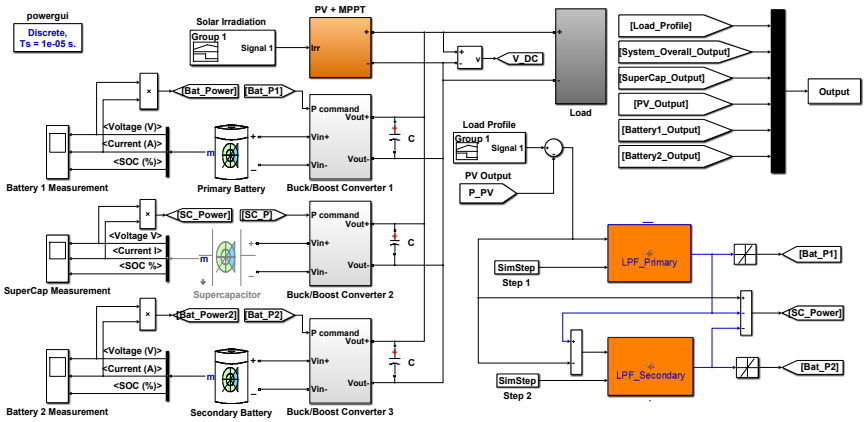

Fig.9. Matlab Simulink model of the proposed HESS.

Li-ion battery type was selected to form the secondary battery due to its superior performance, such as longer cycle life, higher c-rate capability and wider operating SOC range as compared to LA battery. These characteristics is desirable for handling the medium frequency fluctuation in power exchange and the higher cost of Li-ion battery make it a perfect option for the small capacity secondary battery proposed. In this paper, the scaling factor is set as 0.95 and the secondary battery of the proposed HESS will contribute 5 percent (50Ah) to the overall energy storage capacity. Since the main focus of this work is to evaluate the effectiveness of the proposed HESS in mitigating battery stress, the SOC control of the batteries and SC are not implemented and the SOCs of battery and SC are assumed to operate in acceptable range.

Table 1 – System parameters of the Matlab Simulink model.

Parameter	Battery-Only	Passive HESS	Active HESS	Proposed HESS
PV array peak power (kW_p)		5		
Daily load energy consumption (kWh)		27.4		
Battery nominal voltage (V)		48		
Battery capacity (Primary) (Ah)	1000	1000	1000	950
Battery capacity (Secondary) (Ah)	-	-	-	50
Battery internal resistance (ohm)	0.005	0.005	0.005	0.005
SC capacitance (F)	-	1000	1000	1000
SC equivalent series resistance (ohm)	-	0.001	0.001	0.001
Scaling factor W_1	-	-	-	0.95
Time constant (Primary LPF) (sec)	-	-	-	600
Time constant (Secondary LPF) (sec)	-	-	-	300

The analysis will be carried out under different scenarios using actual solar irradiance data and estimated load profiles in rural Sarawak. Fig.10 shows the simulated power profile of a 5KW PV array for a typical sunny and cloudy day recorded in Sarawak, Malaysia.

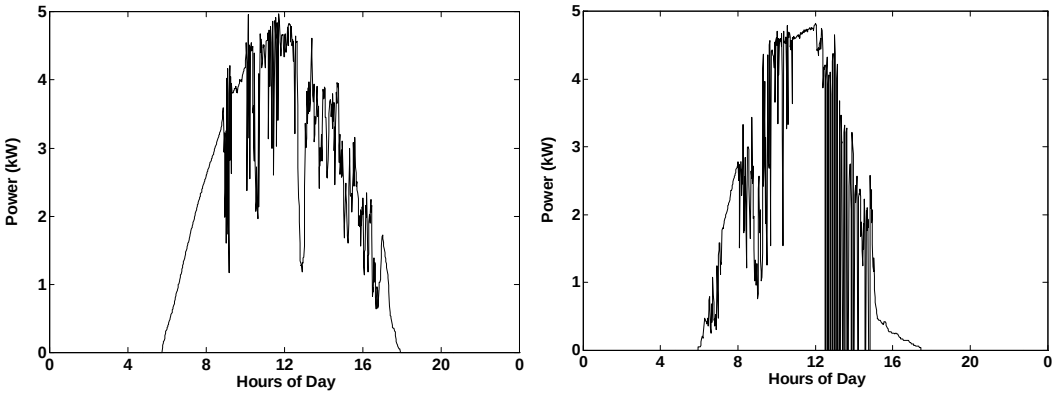

(a) Sunny day (b) Cloudy day

Fig. 10. 5kW PV generation profile of typical weather conditions in Sarawak, Malaysia.

On the other hand, the load profiles used in the simulation analysis were estimated based on actual survey data collected from a rural community in inner part of Sarawak (1˚14'20.5"N, 112˚02'10.7"E). The targeted rural site consists of 6 households and the common electrical appliances are lighting, television, common refrigerator, electric fan and simple electronic devices. Fig. 11(a) presents normal daily electricity consumption, while Fig. 11(b) shows a heavy electricity consumption which could be family day or festive season.

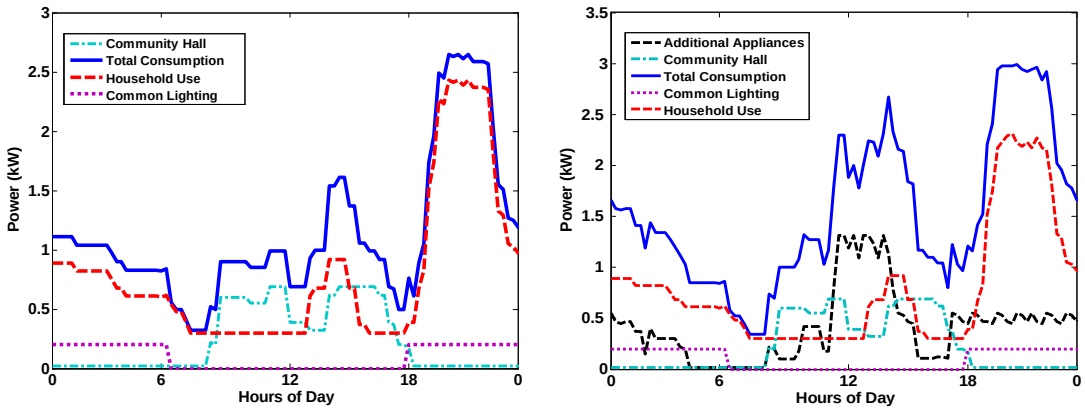

(a) Normal electricity consumption (b)Heavy electricity consumption

Fig. 11. Estimated load profiles of the target rural site in Sarawak, Malaysia.

To evaluate and benchmark the performance of the proposed multi-level HESS and existing HESS schemes with conventional battery-only setting, three scenarios are considered as shown in Fig. 12: (a) sunny day with normal electricity consumption, (b) sunny day with heavy electricity consumption, and (c) cloudy day with normal electricity consumption. To present a fair comparison and benchmarking between the proposed and existing HESS topologies, the Matlab Simulink model of the standalone PV microgrid with battery-only ESS, passive SC-battery HESS and active SC-battery HESS are constructed with identical battery and SC parameters.

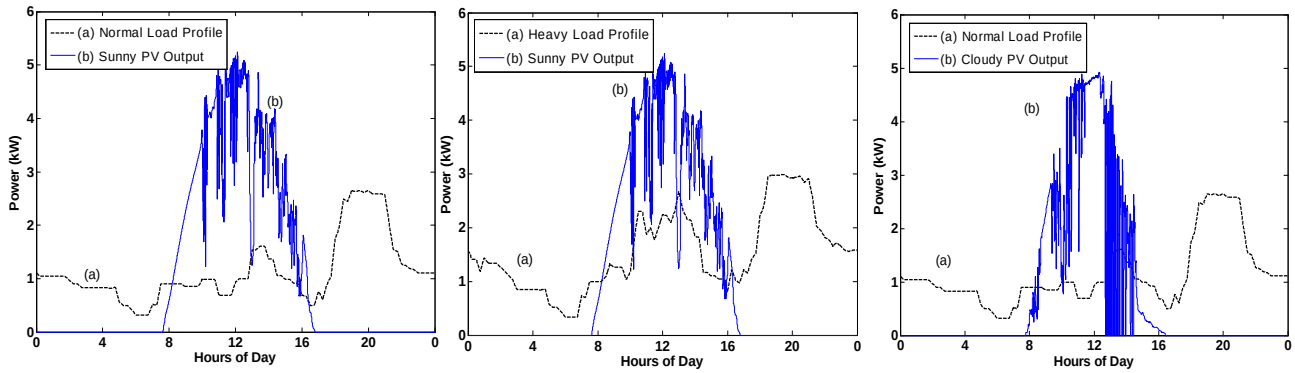

(a) Sunny Day with Normal Load (b) Sunny Day with Heavy Load (c) Cloudy Day with Normal Load

Fig. 12. Simulation conditions used for evaluating the performance of different HESS topologies.

Fig. 13 shows the variations of the battery current in 24 hours for the different HESS topologies and power management strategies considered in this work. As shown in the enlarged view of battery currents (figures on the right), the proposed HESS demonstrated the most stable current to the primary battery as compared to the active HESS, while the smoothing capability of the passive HESS is hardly observable because the time constant of the SC response in within the range of seconds. Also observed from the battery currents is that the peak battery current in the proposed HESS scheme is the lowest among the four topologies under consideration (see Table 2). As for the cycling performance of primary battery, the change in battery state-of-charge does not show significant difference among the different HESS topologies as shown in Fig. 14. This phenomenon is expected as the average power of the low frequency component does not change throughout the day.

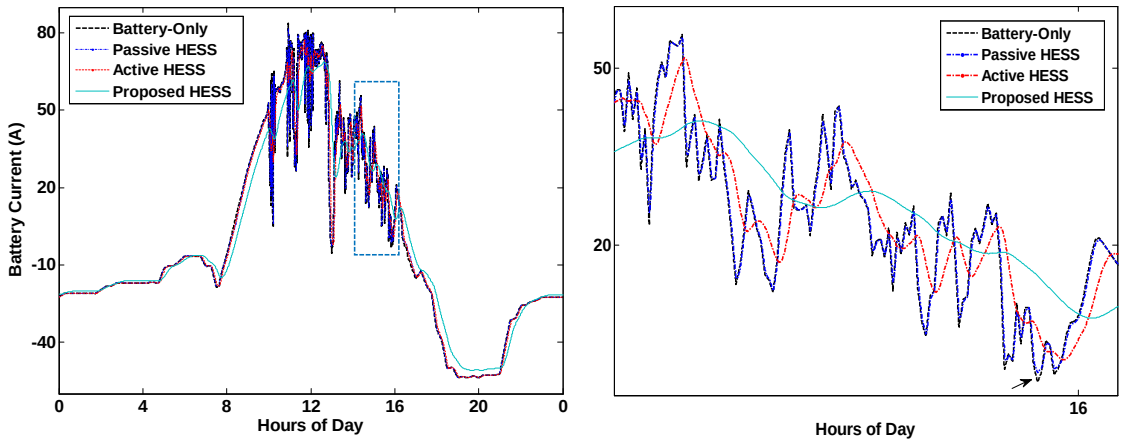

(a) Sunny Day with Normal Load

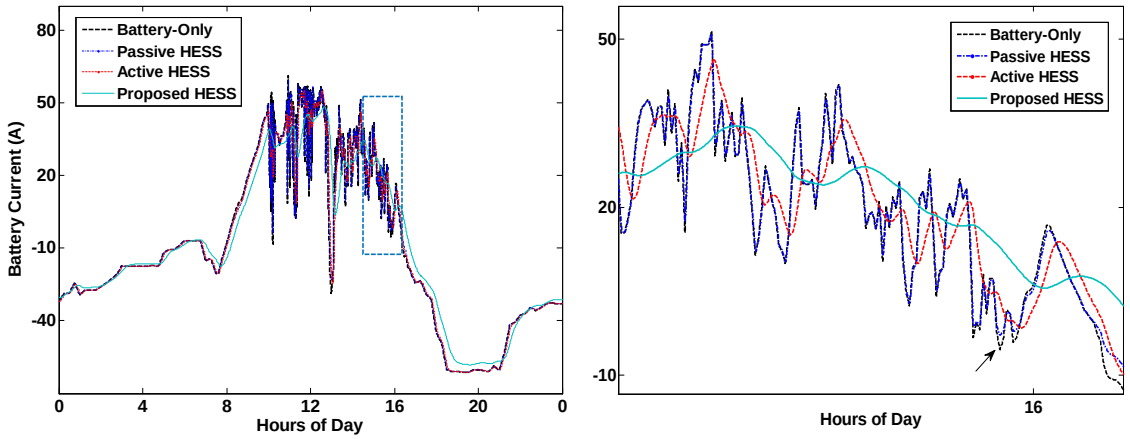

(b) Sunny Day with Heavy Load

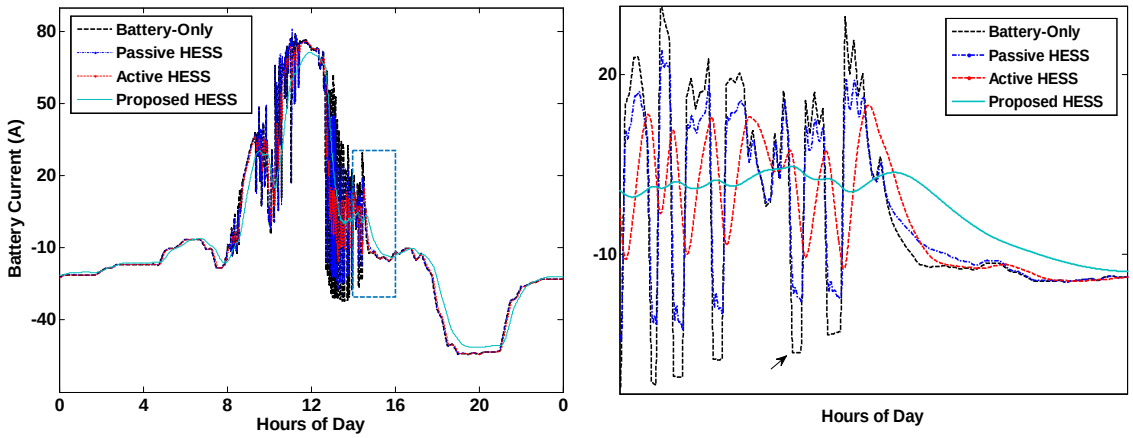

(c) Cloudy Day with Normal Load

Fig. 13. Primary battery current of HESS Topologies under consideration and the coresponding enlarged views on the right.

To evaluate the efficiency in utilization of SC in different HESS topologies, the maximum variations in SC state-of-charge (*max[SoC_SC] – min[SoC_SC]*) are compared as shown in Fig. 15 and Table 2. As expected, the passive HESS has the lowest SC utilization of less than 10 percent as a result of sharing terminal voltage with battery. While the active and proposed HESS topologies have approximately similar SC utilization of about 60 percent. The higher SC utilization rate suggests that the SC is capable of absorbing more high-frequency fluctuation in ESS power exchange, hence mitigating highly dynamic current in battery and also, better cost efficiency.

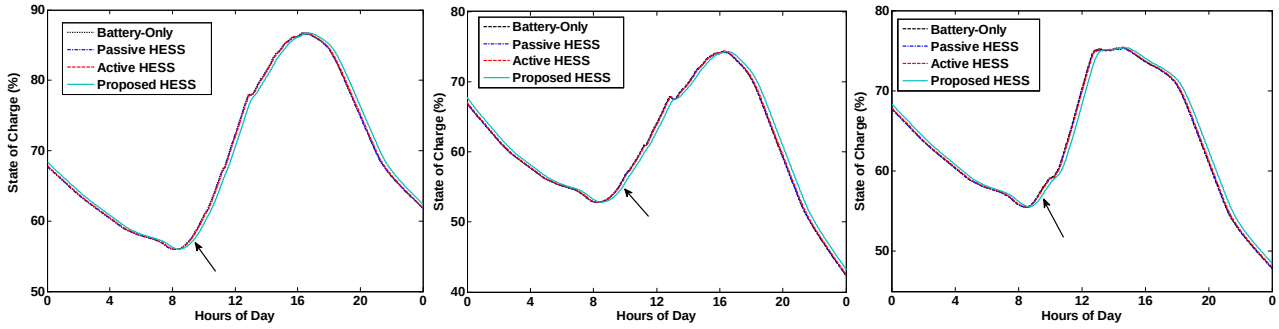

(a) Sunny Day with Normal Load (b) Sunny Day with Heavy Load (c) Cloudy Day with Normal Load

Fig. 14. Primary battery state-of-charge variation throughout the day in three different scenarios.

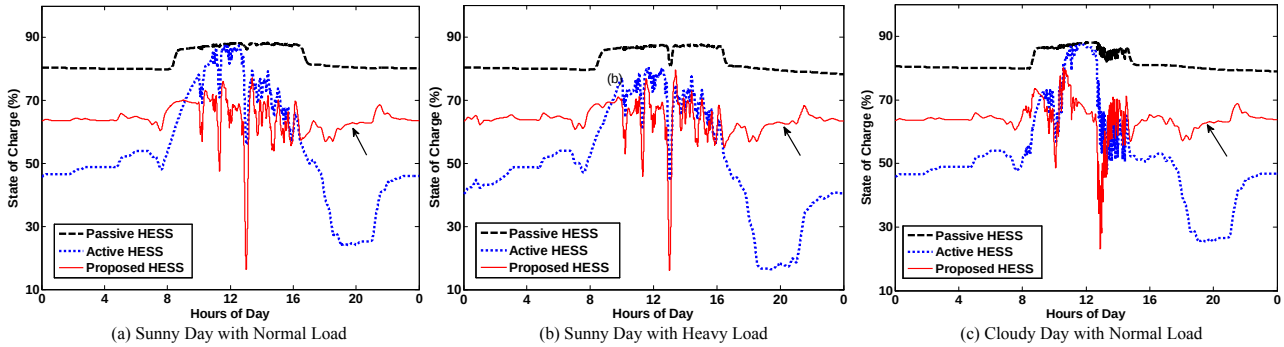

(a) Sunny Day with Normal Load (b) Sunny Day with Heavy Load (c) Cloudy Day with Normal Load

Fig. 15. SC state-of-charge variation throughout the day in three different scenarios.

4. COST ANALAYSIS

In order to validate the effectiveness of the proposed HESS in mitigating charge/discharge stress on battery, a battery health cost function *Cost(T)* is formulated to quantify the impact of battery current on the cycle life of battery as shown [38]:

$$Cost(T) = \sum_{t=0}^{T} n_1[i_b(t)]^2 + n_2\left|\frac{di_b(t)}{dt}\right| + n_3[\max(b(t)) - \min(b(t))]^2 + n_4\begin{vmatrix}1 & ;if\ [i_b(t)\cdot i_b(t-1) < 0]\\ 0 & ;if\ [i_b(t)\cdot i_b(t-1) \geq 0]\end{vmatrix} + n_5 \quad (3)$$

Where T is the total operating time, $i_b(t)$ is the battery current, $b(t)$ is the battery SoC, while n_1, n_2, n_3, n_4 and n_5 are positive constants. Five life-limiting factors are considered: (1) charge/discharge rate, (2) dynamicity of battery current, (3) depth-of-discharge (DoD), (4) charge/discharge transition, and (5) calendar life. The first term quantifies the damaging impact of high charge/discharge current; the second term captures the effect of undesirable fluctuation in battery current; the third term penalizes the impact of deep discharge; the fourth term considers the effect of cycling; and the last term captures calendar life of battery. The health cost of charge/discharge rate and depth-of-discharge are modeled as convex function [39].

In order to benchmark the different HESS topologies to battery-only system, the *Cost(T)* for all systems are normalized based on the battery health cost of battery-only system. Fig. 16 shows the normalized battery health cost of the four HESS topologies under consideration in the three different scenarios. Table 2 summarizes the simulation results presented in Section 3 and the associated battery health cost analysis. The results show that the proposed multi-level HESS demonstrates about 42-46 percent reduction in battery health cost in normal

condition (sunny day), while nearly 70 percent reduction in battery health cost in harsh condition (cloudy day) compared to battery-only system. The proposed HESS performs approximately 11-30 percent more superior than the conventional active HESS which suggests the slowest deterioration rate in battery performance and longest service life under comparable operating condition.

Although the battery aging process is a rather complex phenomenon which cannot be quantified accurately with the simplified battery health cost function used in this work. However, the intention of this analysis is to evaluate and compare relatively the effectiveness of different HESS schemes in mitigating detrimental loading conditions in battery based on the well-understood life-limiting factors. It is assumed that the impacts of life-limiting factors to battery's health are linear and independent.

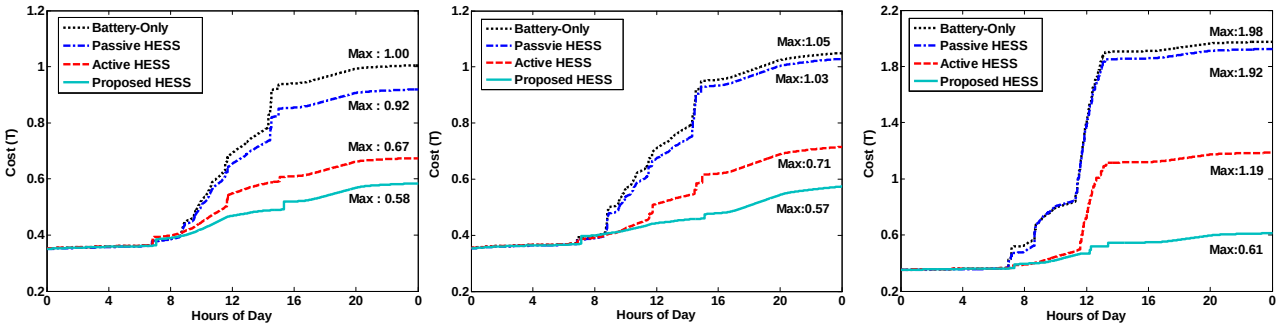

(a) Sunny Day with Normal Load (b) Sunny Day with Heavy Load (c) Cloudy Day with Normal Load

Fig. 16. Primary battery normalized health cost throughout the day in three different scenarios.

Table 2 – Numerical simulation results

HESS Topology	Weather / Load Condition	Maximum Battery Current (A)	Battery Depth-of-Discharge (%)	SC Utilization (%)	Battery Health Cost *Cost(T)*	Percentage *Cost(T)* Reduction[1] (%)
Battery-Only	Sunny / Normal	83.65	30.78	-	1.00	-
	Sunny / Heavy	61.14	31.97	-	1.05	-
	Cloudy / Normal	79.05	27.51	-	1.98	-
Passive HESS	Sunny / Normal	82.02	30.66	9.91	0.92	8.0
	Sunny / Heavy	59.62	31.82	9.54	1.03	1.9
	Cloudy / Normal	81.21	27.39	9.73	1.92	3.0
Active HESS	Sunny / Normal	77.29	30.77	63.97	0.67	33.0
	Sunny / Heavy	54.88	31.78	63.69	0.71	32.4
	Cloudy / Normal	76.21	27.35	62.09	1.19	39.9
Proposed HESS	Sunny / Normal	68.80	30.69(Primary)	60.88	0.58(Primary)	42.0
	Sunny / Heavy	48.35	30.92(Primary)	63.45	0.57(Primary)	45.7
	Cloudy / Normal	71.37	26.79(Primary)	56.93	0.61(Primary)	69.2

#Note 1 – Percentage Cost(T) reduction is calculated in relative to battery-only system.

In order to justify the additional cost of implementing the secondary Li-ion battery module with higher price tag, a financial analysis is presented in Table 3. Assuming the battery's life cycle is linearly proportional to the reciprocal of battery health cost, the estimated life cycle of battery for different topologies are calculated based on the typical life expectancy of 500 cycles for Lead Acid battery and 2000 cycles for Li-ion battery. The secondary battery of the proposed HESS is estimated to last 50 percent of its normal life expectancy due to the fact that this battery will be handling harsh charge/discharge current. Assuming the battery is cycled once a day for the entire year, the estimated battery operating cost per annum is estimated. Based on the financial analysis, despite the addition of secondary battery module of higher cost, the proposed multi-level HESS still managed

to reduce the operating cost of energy storage system by a minimum of 38.4% in gentle condition and 67.5% in harsh condition.

Table 3 – Financial analysis of different HESS

HESS Topology	Weather / load condition[4]	Capacity (kWh)	Initial Cost[3] ($)	Battery Health Cost *Cost()*	Estimated Life Cycle[1]	Cost / Cycle ($)	Estimated Annual Battery Cost ($)	Percentage Cost Reduction[5] (%)
Battery-only	S / N	48	7200	1.00	500	14.40	**5256.00**	**0**
	S / H			1.05	476	15.13	**5522.45**	**0**
	C / N			1.98	252	28.57	**10428.05**	**0**
Passive HESS	S / N	48	7200	0.92	547	13.16	**4803.40**	**8.6**
	S / H			1.03	485	14.85	**5420.25**	**1.9**
	C / N			1.92	260	27.69	**10106.85**	**3.1**
Active HESS	S / N	48	7200	0.67	747	9.64	**3518.60**	**33.1**
	S / H			0.71	704	10.23	**3733.95**	**32.4**
	C / N			1.19	420	17.14	**6256.10**	**40.0**
Proposed HESS								
Primary	S / N	45.6	6840	0.58	865	7.91	2887.15 + 350.40	**38.4**
Secondary		2.4	960	-	1000[2]	0.96	= **3237.55**	
Primary	S / H	45.6	6840	0.57	877	7.80	2847.00 + 350.40	**42.1**
Secondary		2.4	960	-	1000[2]	0.96	= **3197.4**	
Primary	C / N	45.6	6840	0.61	820	8.34	3044.10 + 350.40	**67.5**
Secondary		2.4	960	-	1000[2]	0.96	= **3394.50**	

#Note 1 – Typical life cycle / Cost of battery utilization; typical life cycle for LA – 500 cycles, and Li-ion – 2000 cycles.
#Note 2 – Estimated to perform 50% of the expected cycle life.
#Note 3 – Initial cost of LA battery ($150/kWh) and Li-ion battery ($400/kWh) is considered.
#Note 4 – S – Sunny, C – Cloudy, N – Normal load, H – Heavy load.
#Note 5 – Percentage cost reduction is calculated based on battery-only system.

5. CONCLUSION

Standalone photovoltaic microgrid with energy storage system has been an attractive solution for off-grid communities. Lead acid battery as the mainstream energy storage system for renewable microgrid suffers from low life expectancy which results in poor reliability and high operating cost. Hybridization of energy storage devices with different characteristic and its associated energy management system have been actively researched in quest of enhancing the service life of battery. This paper proposed a novel multi-level HESS configuration and the associated control strategy to mitigate the battery stress under dynamic power exchange condition that often experienced in standalone renewable microgrid. A Matlab Simulink model of typical standalone photovoltaic microgrid is developed to analyze the performance of HESS in stress reduction which leads to service life extension. Different conditions of solar energy input and load profiles from a rural site in Sarawak were used in the simulation and analysis. A battery health cost function is formulated based on selected life-limiting factors to predict the health cost of battery in different HESS topologies. The study results show that the proposed multi-level HESS could effectively mitigate stress on battery with lowest impact on the battery health. This suggests that improvement of battery life can potentially be achieved by using the proposed system. Financial analysis shows that the proposed system is financially viable with no significant increase in overall cost.

REFERENCE

[1] E. H. Van Nes, M. Sche, V. Brovkin, T. M. Lenton, H. Ye, E. Deyle, and G. Sugihara, "Causal feedbacks in climate change," *Nat. Clim. Chang.*, no. March, pp. 3–6, 2015.

[2] P. A. Owusu and S. Asumadu-sarkodie, "A review of renewable energy sources , sustainability issues and climate change mitigation," *Cogent Eng.*, vol. 15, no. 1, pp. 1–14, 2016.

[3] International Energy Agency, “World Energy Outlook 2016,” *IEA*, vol. Chapter 1, 2016.
[4] X. Tan, Q. Li, and H. Wang, “Advances and trends of energy storage technology in Microgrid,” *Int. J. Electr. Power Energy Syst.*, vol. 44, no. 1, pp. 179–191, 2013.
[5] C. Gouveia, J. Moreira, C. L. Moreira, and J. A. Pecas Lopes, “Coordinating storage and demand response for microgrid emergency operation,” *IEEE Trans. Smart Grid*, vol. 4, no. 4, pp. 1898–1908, 2013.
[6] S. Shivashankar, S. Mekhilef, H. Mokhlis, and M. Karimi, “Mitigating methods of power fl uctuation of photovoltaic (PV) sources – A review,” *Renew. Sustain. Energy Rev.*, vol. 59, pp. 1170–1184, 2016.
[7] C. Spanos, D. E. Turney, and V. Fthenakis, “Life-cycle analysis of fl ow-assisted nickel zinc- , manganese dioxide- , and valve-regulated lead-acid batteries designed for demand-charge reduction,” *Renew. Sustain. Energy Rev.*, vol. 43, pp. 478–494, 2015.
[8] R. Dufo-lópez, J. M. Lujano-rojas, and J. L. Bernal-agustín, “Comparison of different lead – acid battery lifetime prediction models for use in simulation of stand-alone photovoltaic systems,” vol. 115, pp. 242–253, 2014.
[9] F. Scuiller, T. Tang, Z. Zhou, M. Benbouzid, and J. Fre, “A review of energy storage technologies for marine current energy systems,” *Renew. Sustain. Energy Rev.*, vol. 18, pp. 390–400, 2013.
[10] A. Lahyani, P. Venet, A. Guermazi, and A. Troudi, “Battery/Supercapacitors Combination in Uninterruptible Power Supply (UPS),” *IEEE Trans. Power Electron.*, vol. 28, no. 4, pp. 1509–1522, 2013.
[11] H. Yin, C. Zhao, M. Li, and C. Ma, “Utility Function-Based Real-Time Control of A Battery Ultracapacitor Hybrid Energy System,” *IEEE Trans. Ind. Informatics*, vol. 11, no. 1, pp. 220–231, 2015.
[12] L. Y. and W. C. Yanzi Wang, Weida Wang, Yulong Zhao, “A Fuzzy-Logic Power Management Strategy Based on Markov Random Prediction for Hybrid Energy Storage Systems,” *Energies*, vol. 9, no. 1, p. 25, 2016.
[13] V. Bolborici, F. p. Dawson, and Ke. K. Lian, “Hybrid Energy Storage Systems:Connecting batteries in parallel with ultracapacitors for higher power density,” *IEEE Ind. Appl. Mag.*, no. April, pp. 31–40, 2014.
[14] W. Jing, C. H. Lai, M. L. Dennis Wong, and W. S. H. Wong, “Smart hybrid energy storage for stand-alone PV microgrid: Optimization of battery lifespan through dynamic power allocation,” *Asia-Pacific Power Energy Eng. Conf. APPEEC*, vol. 2016–Janua, pp. 3–7, 2016.
[15] A. M. Gee, F. V. P. Robinson, and R. W. Dunn, “Analysis of battery lifetime extension in a small-scale wind-energy system using supercapacitors,” *IEEE Trans. Energy Convers.*, vol. 28, no. 1, pp. 24–33, 2013.
[16] M. Choi, S. Kim, and S. Seo, “Energy Management Optimization in a Battery / Supercapacitor Hybrid Energy Storage System,” *IEEE Trans. Smart Grid*, vol. 3, no. 1, pp. 463–472, 2012.
[17] N. Mendis, K. M. Muttaqi, and S. Perera, “Management of Battery-Supercapacitor Hybrid Energy Storage and Synchronous Condenser for Isolated Operation of PMSG Based Variable-Speed Wind Turbine Generating Systems,” vol. 5, no. 2, pp. 944–953, 2014.
[18] S. Adhikari, Z. Lei, W. Peng, and Y. Tang, “A Battery / Supercapacitor Hybrid Energy Storage System for DC Microgrids,” *ECCE Asia*, pp. 8–14, 2016.
[19] M. E. Glavin and W. G. Hurley, “Optimisation of a photovoltaic battery ultracapacitor hybrid energy storage system,” *Sol. Energy*, vol. 86, no. 10, pp. 3009–3020, 2012.
[20] R. A. Dougal, S. Member, S. Liu, and R. E. White, “Power and Life Extension of Battery – Ultracapacitor Hybrids,” *IEEE Trans. COMPONENTS Packag. Technol.*, vol. 25, no. 1, pp. 120–131, 2002.
[21] D. Tran, A. M. Khambadkone, and S. Member, “Energy Management for Lifetime Extension of Energy Storage System in Micro-Grid Applications,” vol. 4, no. 3, pp. 1289–1296, 2013.
[22] H. Zhou, T. Bhattacharya, D. Tran, T. S. T. Siew, and A. M. Khambadkone, “Composite Energy Storage System Involving Battery and UltracapacitorWith Dynamic Energy Management in Microgrid Applications,” *IEEE Trans. POWER Electron.*, vol. 26, no. 3, pp. 923–930, 2011.
[23] S. K. Kollimalla, M. K. Mishra, and N. L. Narasamma, “Design and analysis of novel control strategy for battery and supercapacitor storage system,” *IEEE Trans. Sustain. Energy*, vol. 5, no. 4, pp. 1137–1144, 2014.
[24] S. Dusmez and A. Khaligh, “A Supervisory Power-Splitting Approach for a New Ultracapacitor–Battery Vehicle Deploying Two Propulsion Machines,” *IEEE Trans. Ind. Informatics*, vol. 10, no. 3, pp. 1960–1971, 2014.
[25] A. D. Grasso, C. Sapuppo, G. M. Tina, and R. Giusto, “MPPT charge regulator for photovoltaic stand-alone dual battery systems,” *Electr. Eng. Res. Rep.*, vol. 2, no. 1, 2009.
[26] G. Barca, A. Moschetto, C. Sapuppo, G. M. Tina, R. Giusto, and A. D. Grasso, “A novel MPPT charge regulator for a photovoltaic stand-alone telecommunication system,” pp. 235–238, 2008.
[27] W. Jing, C. H. Lai, S. H. W. Wong, and M. L. D. Wong, “Battery-Supercapacitor Hybrid Energy Storage System in Standalone DC Microgrids : A Review,” *IET Renew. Power Gener.*
[28] M. Bortolini, M. Gamberi, and A. Graziani, “Technical and economic design of photovoltaic and battery energy storage system,” *Energy Convers. Manag.*, vol. 86, pp. 81–92, 2014.
[29] A. Kuperman, I. Aharon, A. Kara, and S. Malki, “A frequency domain approach to analyzing passive battery-ultracapacitor hybrids supplying periodic pulsed current loads,” *Energy Convers. Manag.*, vol. 52, no. 12, pp. 3433–3438, 2011.
[30] J. Shen, A. Khaligh, and S. Member, “A Supervisory EnergyManagement Control Strategy in a Battery/Ultracapacitor Hybrid Energy Storage System,” *IEEE Trans. Transp. Electrif.*, vol. 1, no. 3, pp. 223–231,

2015.
[31] L. Shao, M. Moshirvaziri, C. Malherbe, A. Moshirvaziri, A. Eski, S. Dallas, F. Hurzook, and O. Trescases, "Ultracapacitor/battery hybrid energy storage system with real-time power-mix control validated experimentally in a custom electric vehicle," *2015 IEEE Appl. Power Electron. Conf. Expo.*, pp. 1331–1336, 2015.
[32] T. Ma, H. Yang, and L. Lu, "Development of hybrid battery-supercapacitor energy storage for remote area renewable energy systems," *Appl. Energy*, vol. 153, pp. 56–62, 2015.
[33] A. Etxeberria, I. Vechiu, H. Camblong, and J. M. Vinassa, "Comparison of three topologies and controls of a hybrid energy storage system for microgrids," *Energy Convers. Manag.*, vol. 54, no. 1, pp. 113–121, 2012.
[34] S. Zhang, R. Xiong, and X. Zhou, "Comparison of the topologies for a hybrid energy-storage system of electric vehicles via a novel optimization method," *Sci. China Technol. Sci.*, vol. 58, no. 7, pp. 1173–1185, 2015.
[35] P. Ultra, C. Battery, E. Jamshidpour, P. Poure, and S. Saadate, "Energy Management and Control of a Stand-Alone Photovoltaic/Ultra Capacitor/Battery Microgrid," *2015 IEEE Jordan Conf. Appl. Electr. Eng. Comput. Technol.*, vol. 2, no. 1, pp. 1–12, 2016.
[36] A. L. Allègre, A. Bouscayrol, and R. Trigui, "Influence of control strategies on battery / supercapacitor hybrid Energy Storage Systems for traction applications," pp. 213–220, 2009.
[37] W. Jiang, L. Zhang, H. Zhao, R. Hu, and H. Huang, "Research on power sharing strategy of hybrid energy storage system in photovoltaic power station based on multi-objective optimisation," *IET Renew. Power Gener.*, vol. 10, no. 5, pp. 575–583, 2016.
[38] W. L. Jing, C. H. Lai, W. S. H. Wong, and M. L. D. Wong, "Cost Analysis of Battery-Supercapacitor Hybrid Energy Storage System for Standalone Pv Systems," *4th IET Int. Conf. Clean Energy Technol.*, 2016.
[39] N. Li, L. Chen, and S. H. Low, "Optimal demand response based on utility maximization in power networks," *Power Energy Soc. Gen. Meet.*, pp. 1–8, 2011.